Design and experimental characterisation of a solar dish with small rim angle

Djelloul Azzouzi[1, 2,*], Boussad Boumeddane[3], Abderahmane Abene[4]

[1]Faculty of sciences and technology, University of Khemis Miliana, Algeria

[2]Industrial fluids laboratory, measurements and applications, University of Khemis Miliana, Algeria

[3]Faculty of Engineering Sciences, University of Blida, Algeria

[4]Valenciennes Institute of Sciences and Techniques, University of Valenciennes, France

**corresponding Author: Road of Tissemsilt, University of Khemis Miliana, Algeria. Email: azzouzidjelloul@yahoo.fr , Phone +213773455352*

Abstract

In this study, a description of the geometrical and optical parameters of the designed solar parabolic concentrator is presented. A suitable choice of the aluminium facet sizes has been optimized and applied. The different steps of concentrator design process are implemented in order to obtain an acceptable adherence of the 152 aluminium facets with the concentrator primary surface. It is indicated that the reflective surface is affected by the number of facets. An azimuth-elevation tracking system was realized. In experimental analysis, the concentration ratio, focal length and sunspot size are determined. Results are discussed and indicate that the experimental concentration ratio and that calculated theoretically are in good agreement.

Keywords: Solar parabolic concentrator, Reflective materials, Sun tracking system, Experimental data

1. Introduction

Solar parabolic concentrator is point focus collector which can be achieving high concentration ratios. This optical quality makes it possible to reach high level temperature at

its focal zone. During these latter decades the design of this solar concentrator type were largely investigated in order to improve its optical and thermal efficiencies. However, the realized technological progress in parabolic dish collectors has promoted their use in various industrial fields.

The major application of the solar parabolic concentrators is to generate electrical power through direct conversion by using the Stirling engines. The 10 KWel Eurodish/Stirling unit [1] and the 1.5 MWel dish/Stirling developed by Maricopa solar project in Arizona/USA [2] represent a real prototypes of this electrical generating mode. Thus, the solar dish is used in other technical applications such as; water desalination and distillation [3,4], irrigation [5] and water heating [6,7].

The design of solar parabolic concentrator requires knowledge of its different characteristic parameters and affecting factors as well as the relation exists between them. One of the significant factors in concentrator design process is the suitable choice of the solar reflector materials which represents a determining characteristic of its optical efficiency. Many reflector materials having a high reflectivity and durability have been used in manufacturing of solar parabolic concentrators, such as silver [8], aluminium [9,10], ceramic metallic coating layer [11] and polished stainless steel [12,13]. The solar parabolic size which is characterised by its aperture diameter, depth, focal length and rim angle affects largely the required power output.

Various sizes of solar parabolic dish were carried out through different experimental studies realized by some researchers. Lovegrove et al [14] studied a designed solar dish having an aperture area of 500 m² with 13.4 m focal length able to reach a very high concentration ratio of about 14100. A solar dish with an aperture area of 400 m² has been constructed and characterised in Australian national university [15,16]. Li and Dubowsky [17] realized a large solar dish mirrors with 30 m aperture diameter and 18.1 m focal length. Theoretically, there

are many significant studies and investigations that developed several models and methodology for the design of the solar parabolic concentrator, in order to improve its optical and thermal efficiency [4,18 - 20].

In first part of this work, an analytical development in order to calculate the primary surface of the paraboloidal concentrator was introduced and showed with more details. Then, the description of the various optical parameters is presented. The second part is devoted for the implementation of the solar parabolic concentrator and its tracking system. This last section has been followed by an experimental characterisation of the designed solar dish.

2. Analytical development

2.2. Geometrical description

The paraboloid concentrator schematized in Fig. 1 is described by the system of the two following equations:

$$x^2 + y^2 = 4fz \tag{1}$$

$$z = \frac{r^2}{4f} \tag{2}$$

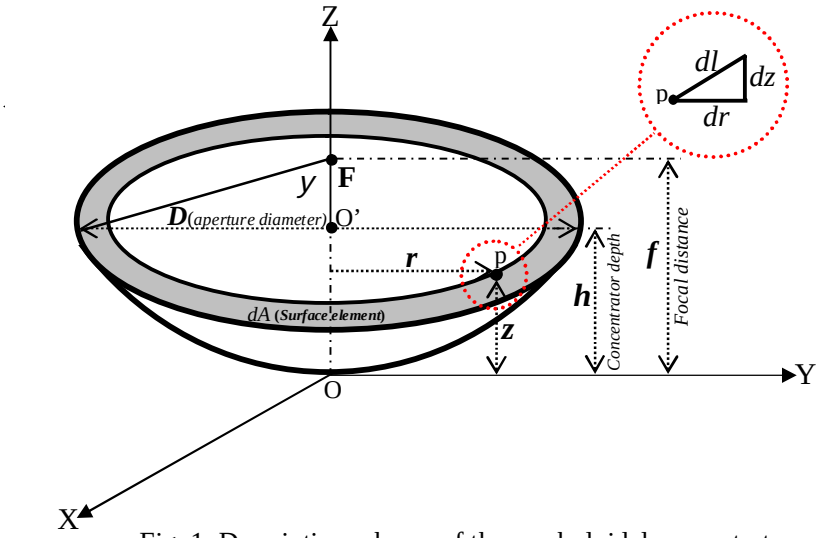

Fig. 1. Descriptive scheme of the paraboloidal concentrator

The determination of the primary surface of a paraboloid concentrator represents an essential step in the geometrical characterization before starting its design. This surface is calculated according to the geometrical parameters chosen beforehand such as: the focal distance f, the aperture diameter D and the concentrator depth h. The surface element dA as indicated in Fig. 1 is expressed analytically as follows:

$$dA = 2\pi r\, dl \tag{3}$$

Where:

$$dl = \sqrt{dz^2 + dr^2}$$

From where:

$$dA = 2\pi r\sqrt{dz^2 + dr^2} \tag{4}$$

Through Eq. (2), the distance element dz is given by:

$$z = \frac{r^2}{4f} \Rightarrow dz = \frac{r}{2f}dr$$

Then Eq. (4) takes the following form:

$$dA = 2\pi r\sqrt{\left(\frac{r}{2f}\right)^2 + 1}\,dr \tag{5}$$

The whole surface A_p of the paraboloid is obtained through the integration of Eq. (5) between 0 and $\frac{D}{2}$ as expressed by Eq. (6).

$$A_p = \int_0^{\frac{D}{2}} 2\pi r\sqrt{\left(\frac{r}{2f}\right)^2 + 1}\,dr \tag{6}$$

Through a variable change $k = \frac{r}{2f}$; ($dr = 2f\,dk$), the Eq. (6) can be taken the following form:

$$A_p = 8\pi f^2 \int_0^{\frac{D}{4f}} \left(k\sqrt{k^2+1}\right) dk \tag{7}$$

A second variable change $t^2 = k^2 + 1$ is used according to Tchebychev conditions [21] applied to the integrals of the differential binominals of type $\int x^n \left(a + bx^n\right)^p dx$. From where; $k = \sqrt{t^2 - 1}$ and $dk = t\left(\sqrt{t^2 - 1}\right)^{-\frac{1}{2}} dt$. When replacing the variable change, the Eq. (7) becomes:

$$A_p = 8\pi f^2 \int_1^{\sqrt{\left(\frac{D}{4f}\right)^2 + 1}} t^2 \, dt \tag{8}$$

After integration, the paraboloidal surface A_p will be given by the following expression:

$$A_p = \frac{8}{3}\pi f^2 \left[\left(\frac{D}{4f}\right)^2 + 1\right]^{\frac{3}{2}} - 1 \tag{9}$$

It should be noted that, the focal length f of the parabolic concentrator and its rim angle γ are given respectively as:

$$f = \frac{D^2}{16H} \tag{10}$$

$$\tan\gamma = \frac{f/D}{2(f/D)^2 - \frac{1}{8}} \tag{11}$$

2.2. Optical description

The dominant parameter to be described in this part is the solar concentration ratio C which represents one of the most important parameters in solar concentration. It is defined as the focused flux at the focal zone, normalized to direct normal insolation. It should be noted that

the peak and mean solar concentration ratio for an ideal paraboloidal concentrator [22,23] are given in Eqs. (7) and (8) respectively:

$$C_{peak} = \frac{4}{q^2} \sin^2(\gamma) \tag{12}$$

$$C_{mean} = \frac{\sin^2(\gamma)\cos^2\left(\gamma + \frac{q}{2}\right)}{\sin^2\left(\frac{q}{2}\right)} \tag{13}$$

Where, q is the solar disc angle has an average value of about 0.00931 radian. (From 0.00948 radian in January to 0.00917 radian in July).

By a simple derivation of the Eq. 13, it results that $\frac{dC_{mean}}{d\gamma} = 0$ at $\gamma \approx 45°$. This result shows that the mean concentration ratio is maximized for a paraboloidal concentrator which having a rim angle of about 45°. However, the solar image (sunspot) focused through a perfect solar paraboloidal concentrator with a plate receiver placed at its focal zone takes a circular form [22] with a diameter equal to $f\,q$. Through the study of Schmidt et al [24], it shows that the maximal solar concentration ratio to be reached does not depend only on the concentrator rim angle, but as well of the receiver form. Actually, for a spherical receiver, the peak concentration ratio of the paraboloidal concentrator is obtained for 90° rim angles [25].

3. Paraboloidal concentrator design

The designed solar concentrator has an aperture diameter of 1.46m, aperture area of 1.67 m², depth of 25.3 cm and a rim angle of 69.5°. The first step in its conception consists in dividing of the primary surface into eight equal petals. This step is followed by a fine polishing operation of the surface previously divided. Then, the suitable choice of the size of reflecting aluminium facets is carried out in order to ensure a good surface distribution. It is significant

to note that the facet final sizes such as illustrated in Fig. 2 were adopted after several combinations on the all paraboloidal rows. In Table 1 are indicated the type of facet, its numbers by row, surface of each facet as well as the total surface of different paraboloidal rows.

.

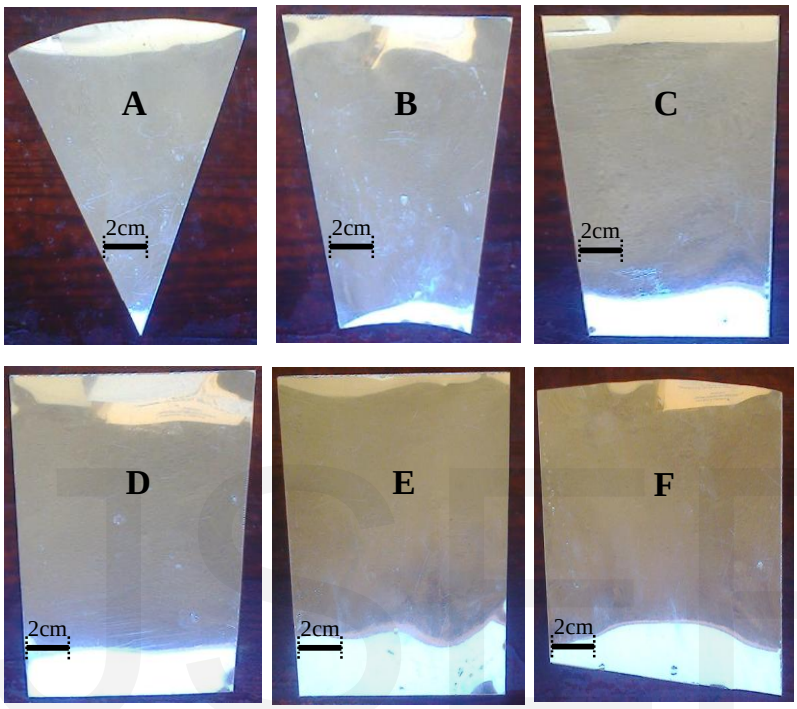

Fig. 2. View of various aluminium facets used in recovering of paraboloid primary surface.

Table 1. Number and surface of each facet type of the reflective concentrator surface.

Row	Facet type	Facets number	Facet surface (cm^2)	Row surface (cm^2)
1	A	8	50.52	404.16
2	B	16	88.39	1414.24
3	C	32	80.36	2571.52
4	D	32	107.55	3441.60
5	E	32	147.72	4727.04
6	F	32	163.01	5216.32
Total reflective surface of the paraboloidal concentrator (cm^2)				17774.88

The high reflectivity of about 0.94 of the used polished aluminium makes it possible to obtain a good optical performances [26] of the designed solar paraboloidal. The second step which is devoted to joining of the various facets has a great importance in all process design. In this last step, perfect adherence between the aluminium facets and the primary surface of the solar paraboloidal are the most required parameter to reach.

Fig. 3 shows a complete sight of the realized solar paraboloidal concentrator on which appeared a diagram illustrating the position of each facet on the primary surface of the petal.

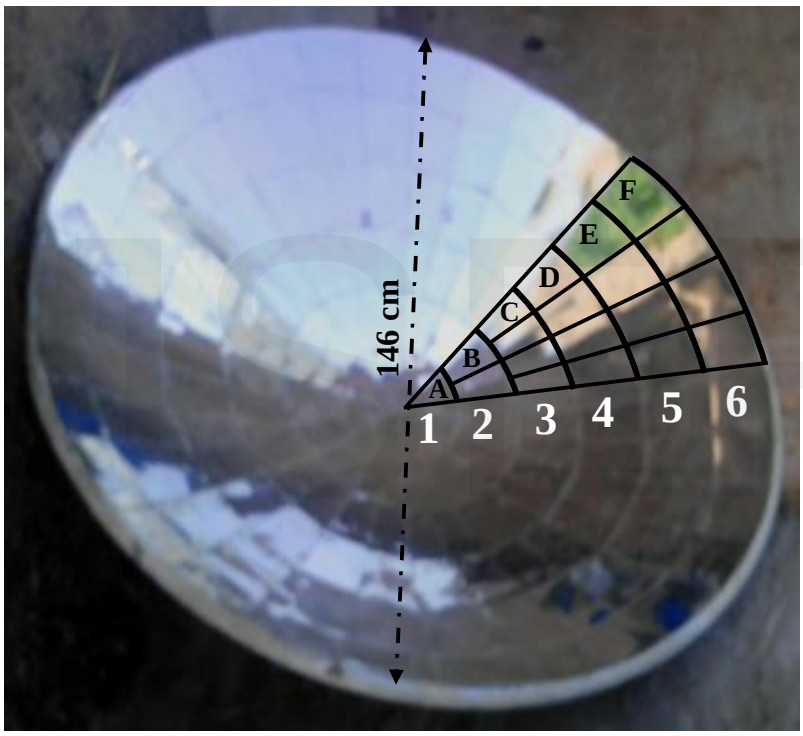

Fig. 3. Photograph of the reflective surface of the solar paraboloidal concentrator.

4. Experimental analysis

In order to carry out the experimental characterisation of the designed solar dish, a solar tracking mechanism was developed especially to ensure the concentrator positioning. Moreover, it makes possible to follow the sun in order to collect as much energy as possible. As shows in Fig. 4 (a) the type of the realized mechanism is an azimuth-elevation tracking. At

its higher end is placed the paraboloidal concentrator which can be freely directed in azimuth and latitude plans. The first experimental test of the solar dish consists to determine its real focal distance.

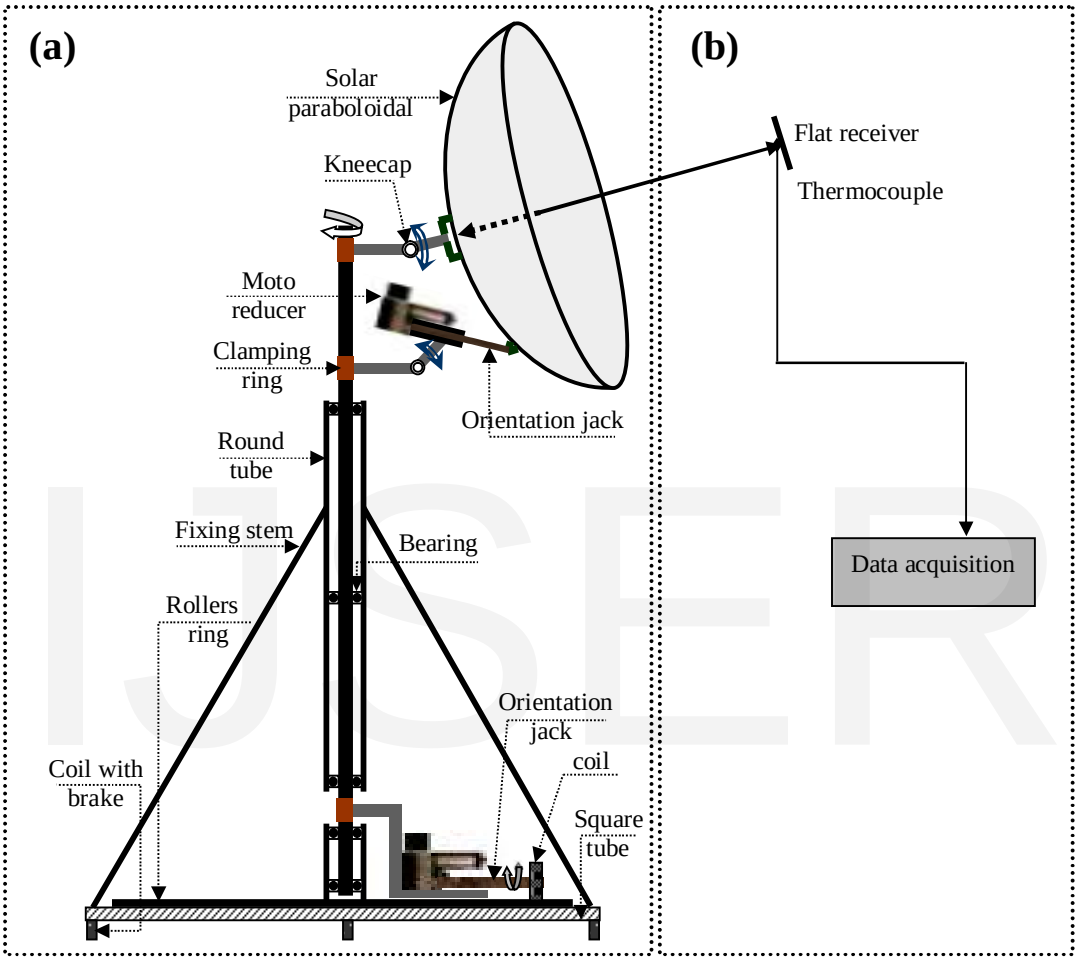

Fig. 4. The realized test bench (a) Tracking mechanism. (b) Schematic of the temperature measurement at the focal point.

In order to carry out this measurement stage, a positioning mechanism along the principal paraboloidal axis as indicated in Fig. 4 (b) has been used. At the upper part, a flat metal receiver is placed on which a thermocouple of type K (-50°C to1200°C) is connected exactly at its center. Then the solar concentrator is directed under an angle of 36° [27] which corresponds to the experimentation site latitude located at Khemis Miliana University, Ain

Defla (Algeria). It is should be noted that the experimental tests were proceeded under a direct normal insolation of 836W/m^2 measured by the CMP11Pyranometre. The temperature of the receiver flat center is measured at various distances from 41cm to 55 cm with a variable step between 3cm to 0.75cm. The maximum value of the temperature is reached when the center of the receiver flat coincides exactly with the focal point.

The second part is devoted to the determination of the real solar concentration ratio which is calculated [28] through the Eq. (14).

$$C = \frac{A_o}{A_s} \tag{14}$$

The focused sunspot surface A_s can be determined by the delimitation of its border which appears on the receiver flat.

5. Results and discussion

The sum of the various surface facets as illustrated in Table 1 gives a total reflective surface of about 1.77 m^2. It is noticed that starting from the third row , more we move away from the basic center of the concentrator, more than the facets size increases in order to obtain the best adherence possible between each facet and primary surface. Moreover, it is noted that the increase in facets number induces a reduction in reflective surface [29] of the solar paraboloidal. This observation can be explained by the significant number of existing gaps between the stuck facets. It appears clearly that reflective surface records a decrease of 4.3 % compared to the primary surface calculated through the Eq. (9) which gives a value of 1.85 m².This difference is simply due to the existing inter-facets junctions. Fig. 9 presents the measured temperatures at various positions of the flat receiver under a direct normal insolation (DNI) of 836 W/m². It appears that the temperature increases up to its maximum of about 1120°C reached at a distance of 52.75 cm which indicates the focal zone. This distance

corresponds exactly to the real focal length of the solar paraboloidal concentrator. The insignificant difference of 1mm between the theoretical focal length and that determined in experiment explains the good adherence obtained during joining operation. The solar image formed at the focal zone takes an elliptical form with a surface of 4.15 cm².

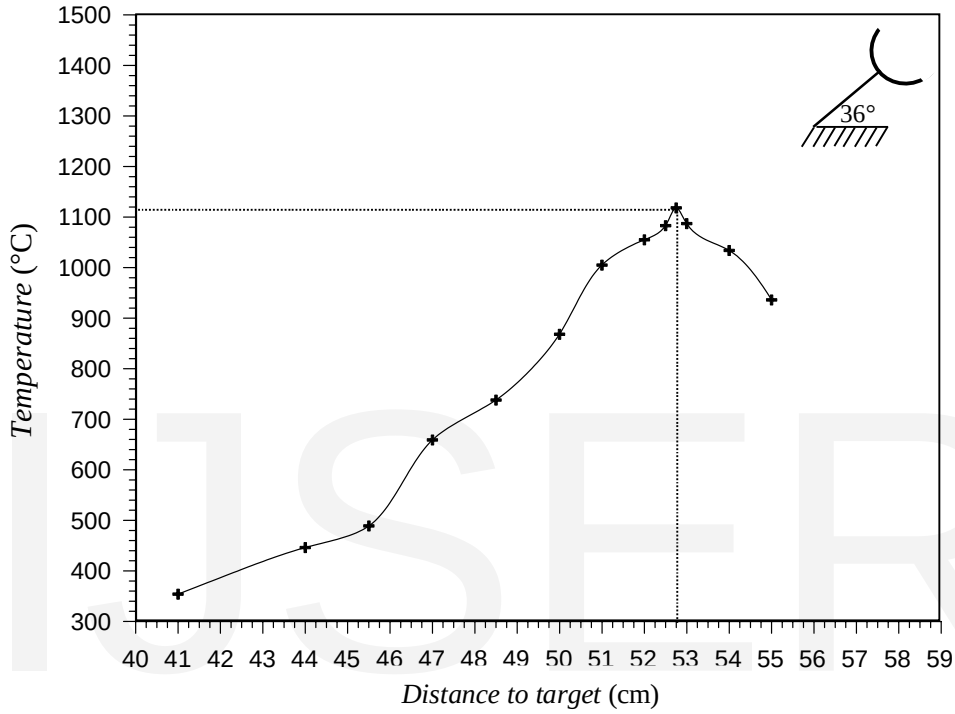

Fig. 5. Measured temperature at various receiver positions along the focal axis.

By applying of the Eq. (14), it results that the real concentration ratio *C* of the solar dish is of about 4021sun, while its mean concentration ratio calculated through the Eq. (13) is equal to 4920sun which gives a difference of 18%. This result shows the good agreement between the concentration ratio determined in experiment and that analytically calculated.

Fig. 6 (a) shows the simulation scheme of the incidental rays at the focal zone using the Soltrace code which presents a very powerful tool to solve the heat flux distribution [30] of solar concentrators and receiver systems.

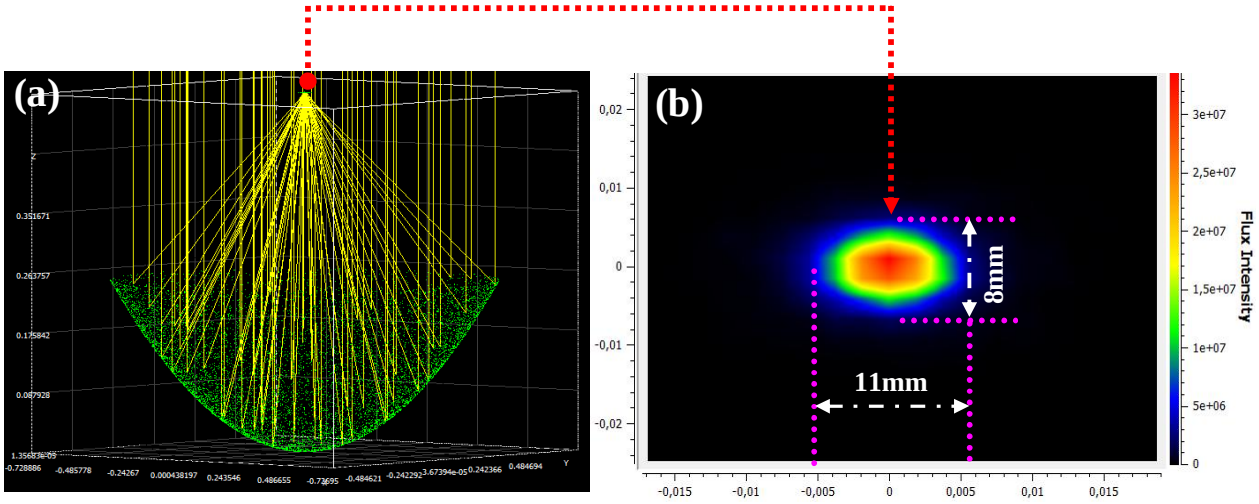

Fig. 6. Soltrace simulation; (a) Incidental rays concentration at the focal zone (b) Flux distribution at the focal zone under a direct normal irradiation of 836W/m².

Referring to the Fig. 6 (b), we observe that the solar image formed at the paraboloidal focal zone takes an elliptical form which has a major and a minor of 8mm. The average flux at the focused solar image is of about 0.16MW/m².

6. Conclusion

The design process of solar parabolic concentrator with small rim angle has been presented in this paper. Through the results analysis, it appears clearly that the decrease in reflective surface compared to the concentrator primary surface can be explained by the existing junctions between facets. Moreover, the suitable size of the various reflective facets and their perfect adherence with the primary surface present a significant role in optical efficiency of the solar dish. It was found that the focal length determined in experiments is very close to that analytically calculated. The difference of about 18% between the experimental concentration ratio and that analytically calculated proves a good implementation of the designed solar dish.

Acknowledgements

This work was supported by the laboratory of Industrial fluids, measurements and applications of Khemis Miliana University, Ain Defla, Algeria.

References

[1] Nepveu, F., Ferriere, A., Bataille, F., 2009. Thermal model of a dish/Stirling systems. Sol Energy 83(1), 81-9.

[2] ⟨ http://www.nrel.gov/csp/solarpaces/⟩ .

[3] Srithar, K., Rajaseenivasan, T., Karthik, N., Periyannan, M., Gowtham, M., 2016. Stand alone triple basin solar desalination system with cover cooling and parabolic dish concentrator. Renew Energy 90, 157–65.

[4] El-Kassaby, MM., 1991. New solar cooker of parabolic square dish: design and simulation. Renew Energy 1(1), 59–65.

[5] Saini Anish, Kohli Shivam, Pillai Ajesh, 2013. Solar powered Stirling engine driven water pump.IJRET 2(11), 615–20.

[6] Dafle, VR. and Shinde, NN., 2012. Design, Development & Performance Evaluation Of Concentrating Monoaxial Scheffler Technology For Water Heating And Low Temperature Industrial Steam Application. Int J Eng Res Appl (IJERA) 2(6), 848–52.

[7] Mohammed, IL. 2012. Design and development of a parabolic dish solar water heater. Int J Eng Res Appl, 2:1.

[8] Mohamed, FM., Jassim, AS., Mahmood, YH., Ahmed, MA., 2012. .Design and study of portable solar dish concentrator. Int J Recent Res Rev (3), 52–9.

[9] Kennedy, CE., Smilgys, RV., Kirkpatrick, DA., Ross, JS., 1997. Optical performance and durability of solar reflectors protected by analumina coating. Thin Solid Films 304(1), 303–9.

[10] Kennedy, CE. and Terwilliger, K., 2005. Optical durability of candidate solar reflectors. J Sol Energy Eng 127(2), 262–9.

[11] Jaworske, DA. and Raack T., 2004. Cermet coatings for solar Stirling space power.Thin Solid films 469, 24–30.

[12] ⟨ www.mirroredstainlesssolutions.com⟩ .

[13] Alarcón, JA., Hortúa, JE., Lopez, A., 2013. Design and construction of a solar collector parabolic dish for rural zones in Colombia. Tecciencia 7(14):14–22.

[14] Lovegrove, K., Burgess, G., Pye, J., 2011. A new 500 m² paraboloidal dish solar concentrator. Solar Energy 85, 620–626.

[15] Johnston, G., 1995. Flux mapping of the 400m² "Big Dish" at the Australian National University. J Sol Energy Eng 117(4), 290-3.

[16] CADDET., 1999. Solar thermal demonstration system with a large paraboloidal dish concentrator. Tech Broch No:105.

[17] Li, L. and Dubowsky, S., 2011. A new design approach for solar concentrating parabolic dish based on optimized flexible petals. Mech Mach Theory 46 (10), 1536–48.

[18] Xu, G., Wang, Y., Quan, Y., Li, H., Li, S., Song, G., Gao, W., 2015. Design and characteristics of a novel tapered tube bundle receiver for high-temperature solar dish system. Appl Therm Eng 91, 791–9.

[19] Ma, H., Jin, G., Zhong, X., Xu, K., Li, Y., 2012. Optical Design of a Solar Dish Concentrator Based on Triangular Membrane Facets. Int J Photo 2012,1–5.

[20] Zhan, WB., Xu, GQ., Quan, YK., Luo, X., Li, TT., 2013. Design and Analysis of a Novel Hybrid Solar/Gas Dish Stirling System (HS/GDSS). Appl Mech Mater; 479–480, 575–9.

[21] Demidovich, B., 1977. Receuil d'exercices et de problèmes d'analyse mathématique. Edition Mir.

[22] Bliss, R.W., 1957. Notes on performance design of parabolic solar furnaces. Solar Energy 1, 22–29.

[23] Rabl, A., 1976. Comparison of solar concentrators. Solar Energy 18, 93-111.

[24] Schmidt, G., Schmid, P., Zewen, H., Moustafa, S., 1983. Development of a point focusing collector farm system. Solar Energy 31, 299–311.

[25] Hernandez, N., Riveros-Rosas, D., Vengas, E., Dorantes, R.J., Rojas-Moran, A., Jaramillo, O.A., Arancibia-Blunes, C.A., Estrada, C.A., 2012. Conical receiver for a paraboloidal concentrator with large rim angle. Solar Energy 86, 1053-1062.

[26] Thomas, F., Gary, J., Harald, K., 2000. Applicability of highly reflective aluminium coil for solar concentrators. Solar Energy 68, 361-370.

[27] Azzouzi, D., Boumeddane, B., Abene, A., 2017. Experimental and analytical thermal analysis of cylindrical cavity receiver for solar dish. Renewable Energy 106, 111-121.

[28] Collares-pereira, M., Gordon, J. M., Rabl, A., Winston, R., 1991. High concentration two-stage optics for parabolic trough solar collectors with tubular absorber and large rim angle. Solar Energy 47, 457- 466.

[29] Riveros-rosas, D., Sanchez-Gonzalez, M., Arancibia-Blunes, C.A., Estrada, C.A., 2011. Influence of the size of facets on point focus solar concentrators. Renewable Energy. 36, 966-970.

[30] NREL. Parabolic trough technology models and software tools. Available: http://www.nrel.gov/csp/troughnet/models_tools.html#soltrace; 2012.

Nomenclature

A_p: paraboloid primary surface (m^2)

A_o: concentrator aperture area (m^2)

A_s: sunspot area (m^2)

C: concentration ratio

C_{peak}: maximal concentration ratio

C_{mean}: mean concentration ratio

D: aperture diameter (m)

f: focal length (m)

h: concentrator depth (m)

T: temperature (K)

x, y: spatial coordinates (m)

Greek symbols

q: solar disc angle (rad)

y: rim angle (rad)

IJSER